RAPID COMMUNICATIONS

PHYSICAL REVIEW B VOLUME 47, NUMBER 19 15 MAY 1993-I

Cyclotron trapping, mode spectroscopy, and mass enhancement in small GaAs/$Al_xGa_{1-x}As$ rings

J. Liu
Department of Physics and Astronomy, The University of North Carolina at Chapel Hill, Chapel Hill, North Carolina 27599-3255

K. Ismail
Department of Telecommunication and Electrical Engineering, University of Cairo, Cairo, Egypt and IBM Thomas J. Watson Research Center, Yorktown Heights, New York 10598

K. Y. Lee and J. M. Hong
IBM Thomas J. Watson Research Center, Yorktown Heights, New York 10598

S. Washburn
Department of Physics and Astronomy, The University of North Carolina at Chapel Hill, Chapel Hill, North Carolina 27599-3255

(Received 10 February 1993)

A new electronic trapping effect has been observed in a small GaAs/$Al_xGa_{1-x}As$ ring, which takes place when the cyclotron orbits match the loop geometry. The trapping causes peaks in the magnetoresistance $R(B)$ at low fields, and the peak positions were used to study the dispersion relation $E_n(k)$ of the one-dimensional magnetoelectric subbands. This allows the ring to be used as a mesoscopic mass spectrometer. The electron effective mass increases with magnetic field by a factor of 50 at field of 0.5 T. General agreement obtains between the experiment and the subband calculations for one-dimensional channels, indicating that true solid-state interferometers are possible.

In 1897, Thompson[1] invented the mass spectrometer, which was later refined by Bainbridge[2] and others. Mass spectroscopy involves bending the trajectory of particles emitted from a point source with a magnetic field and using a point collector to select a particular orbit size, $l_c = mv/eB$. Conventional electron focusing in the solid state is analogous to this magnetic focusing of electrons in vacuum. A magnetic field is used again to focus the electrons injected by a point contact into a second point contact a distance L away.[3] In the conventional mass spectrometer, the momentum of the particle is fixed by an external electric field that accelerates the particle, but in the solid-state experiments, the Fermi energy determines the velocity.[3] The focusing condition is that the cyclotron orbit diameter $2l_c$ be an integer fraction of L, $L = 2jl_c = 2j\hbar k_F/eB$, where $j-1$ is the number of specular bounces of the electron trajectory against the wall between the two point contacts.[4,5] A different experiment, which is more closely related to our work, studied resistance peaks caused by cyclotron orbits pinned to arrays of obstacles whose spacing was commensurate with the orbit size.[6] Both of the above experiments studied transport in large area regions.

Now consider electrons confined to move in circular tracks[2] such as the loop[7] depicted in the inset of Fig. 1. When the cyclotron radius matches the loop radius r, the electrons in the ring experience a kind of cyclotron trapping, or cyclotron resonance, effect, which causes peaks in $R(B)$. The experimental data suggest that the subband modes in the one-dimensional (1D) channel seem *not* to mix with one another, so if n transverse modes are occupied in the loop, then n different values of velocity parallel to the wire cause n peaks in $R(B)$ as each successive l_{cn} matches r.[8] At present, the exact cause for this effect is not yet clear. Based on the established theory of magnetoelectric subbands,[9,10] the motion of the electrons inside the circular channel can be understood, with and without the magnetic field.[9] We speculate that the trapping arises in the area where the ring joins the outlet port. One possibility is that when $l_{cn} = r$, the electrons in mode n are steered away from the outlet port; as a result, the resistance is enhanced and a trapping peak appears. A similar "billiard" description has been used

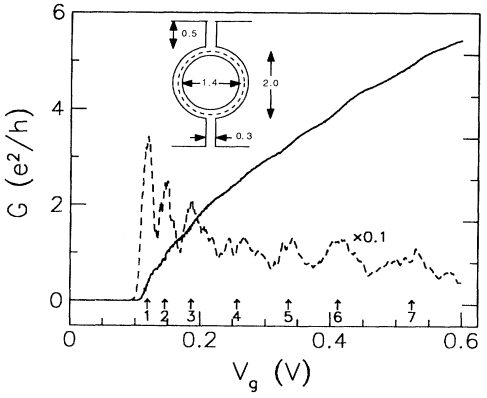

FIG. 1. The inset is a schematic for the sample with dimensions in μm. The dashed line illustrates the trapped orbits. Conductance vs gate voltage is shown for the ring. The turn-on voltages for the modes are determined from dG/dV_g (dashed line) and marked by arrows.

to explain the quenching of Hall resistance and bend resistance in ballistic junctions in the same field range[11] and has proved to be valid for single modes in computer simulations.[12] This classical description can be extended to higher field in the calculation of Hall resistance.[13] If our speculation is right, it may not be necessary to require global ballistic transport around the ring (at this temperature the elastic mean free path in the starting materials is 4.7 μm—roughly equal to the loop circumference of 5.3 μm), rather, we only need well-defined momenta for the electrons approaching the outlet port.

Our samples were fabricated on a standard high-mobility $GaAs/Al_xGa_{1-x}As$ modulation-doped layer (carrier density $n_s = 2 \times 10^{15}/m^2$ and mobility $\mu = 90$ $m^2/V\,sec$) grown by molecular-beam epitaxy. The ring geometry was defined by a shallow mesa formed through a wet etching technique, and a metal gate covers all active portions of the device. More details of the fabrication are reported elsewhere.[7] The ring has a radius $r = 0.85$ μm and linewidths $t = 0.3$ μm. Earlier experiments on similar samples showed clear conductance quantization[14,15] and large Aharonov-Bohm oscillations.[7] Such evidence assures us that the transport in the loops approaches the ballistic regime. All experiments reported here were conducted at $T = 4.2$ K with a standard four-probe lock-in method.

Figure 1 shows the conductance G as a function of gate voltage V_g at $B = 0$ for the ring. Mode counting conductance steps are apparent. The average heights of the steps are $0.75e^2/h$, which is consistent with previous experiments.[7] This value is larger than classical addition of the conductance $2e^2/h$ of independent electron guides (two ports and two ring arms), which would be $0.5e^2/h$. The step heights are regularly spaced. These two facts imply that the modes with the same index are correlated in the arms and the ports, and that the mixing between different index modes is limited. Further study of the mode coupling between straight ports and the ring may provide more clues to the exact cause of the trapping effect, but evidence from bend resistance experiments[11] makes the trapping discussed above very plausible. We also show where the subband bottoms $E_n(0,0)$ cross E_F in the single ring, as determined by the peaks in derivative dG/dV_g.

Figure 2 contains $R(B)$ for the single ring, which contains a series of peaks on a smooth background. [We have noticed similarly peaked $R(B)$ data in the results of others' experiments, too.[16]] We are interested in the focusing peaks, so we have subtracted the smooth part of $R(B)$. We are not sure of the origin of the large negative $R(B)$, but we speculate that it results from steering the incoming beam away from head-on collision with (and strong reflection from) the inner wall of the loop. We used a quasi-Lorentzian functional form,

$$R(B) = R_0 - \Delta/[1 + (B/B_c)^{2.3}] \quad (1)$$

to fit $R(B)$ (dashed line). The power 2.3 is chosen simply because it gives us the best fit, but the results discussed below do *not* depend on this choice. Since the focusing effect at the outlet port increases the resistance,

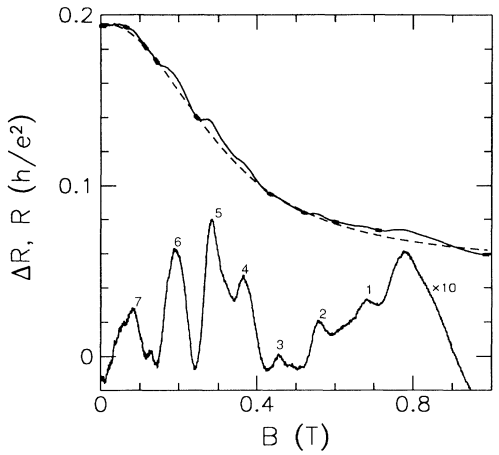

FIG. 2. $R(B)$ the ring at $V_g = 0.55$ V (solid line), is fit to (1) (dashed line), which accounts for the smooth background. The difference between the two, δR, results from orbit trapping.

we only used the low-resistance portions (heavy lines) in the fit, allowing both Δ and B_c as free parameters. After subtracting the smooth part, we nominally have the net contribution of the focusing, which contains several peaks. In addition, one sees the onset of Shubnikov–de Haas (SdH) oscillations (~ 0.5 to ~ 1 T). Peak positions are mapped by fitting a Gaussian function,

$$\Delta R = Ie^{-[(B-B_0)/\Delta B]^2} + aB + c \quad (2)$$

to the data in the neighborhood of each peak, where the last two terms allow for imperfect subtraction and overlap of the peaks. The resulting center field B_0 yields the peak position.

Starting with the relation $l_c = \hbar k_F/eB$, one can show that the cyclotron effective mass is $m_{cn} = \hbar^2 k/(dE_n/dk)$, and tangential (group) velocity is $v_n = dE_n/\hbar\, dk$.[17] The cyclotron trapping condition becomes $r = l_{cn} = \hbar k_{Fn}/eB$, which is the same form as the conventional focusing in free space, but with the Fermi wave vector k_{Fn} *tangential to the arm of the loop.* This allows us to infer k_{Fn} from the peak positions. After measuring $E_F(V_g)$ via the SdH effect ($0 < B < 6$ T) to be $E_F = 5.98V_g + 12.4$ (meV), we have the dispersion relation directly. Figure 3 contains E_F as a function of peak position B_0 (upper axis) and (through the focusing condition) the corresponding wave vectors (lower axis) in convenient units $2\pi/r$. Data from $n = 1$ are omitted because they are sensitive to the functional form (1).

There have been some calculations of the $E_n(k)$ for curved channels[18] in discussions of possible bound states when the radius of curvature is of order $1/k_F$, and there have been quite a few calculations for the straight channels.[15] Since the ring radius is at least one order of magnitude larger than the Fermi wavelength (notice the order of magnitude on the lower abscissa for Fig. 3), we will use the more transparent results for straight channels. A good model of the electrostatic confinement potential comprises a flat bottom plus parabolic walls,[19,9]

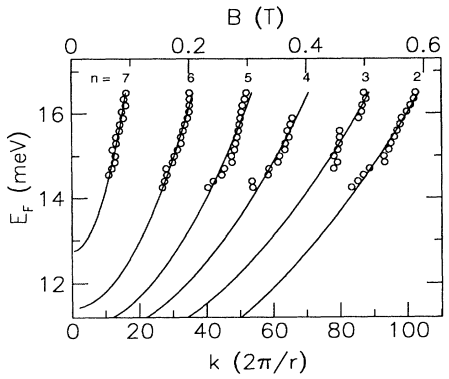

FIG. 3. The focusing peak positions for subband indices 2–7. The solid curves are fits to (3) treating m^* and E_{noff} as free parameters.

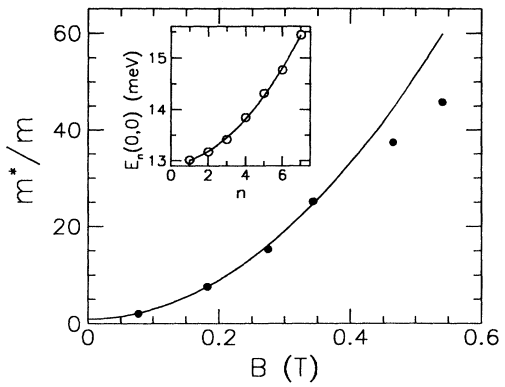

FIG. 4. m^*/m from Fig. 3 as a function of the average magnetic field for each subband. At low field, it fits well with a parabolic function (solid line). The inset contains the zero field subband bottom energy as a function of the band indices n. The solid curve is a least-square fit to the square-well prediction.

$V(|x| > t/2) = m\omega_0^2(|x| - t/2)^2/2$ and $V(|x| < t/2) = 0$, where $m = 0.067m_e$ is the effective mass for two-dimensional GaAs/Al_xGa_{1-x}As (100) electron gas. At $B = 0$, the problem has been solved analytically[20] with the result

$$E_n(k,0) = E_n(0,0) + \hbar^2k^2/2m, \tag{3}$$

where the energy of the subband bottom is

$$E_n(0,0) = E_P\{[(2n+1) + E_P/E_S]^{1/2} - [E_P/E_S]^{1/2}\}^2 \tag{4}$$

and $E_S = (\pi\hbar)^2/2mt^2$ and $E_P = \hbar\omega_0/2$ are ground-state energies for square (width t) and parabolic wells, respectively. The effective mass is not changed by the electrostatic confinement.

Now we can compare the measured $E_n(0,0)$ from Fig. 1 ($B = 0$) with these formulas as shown in the inset of Fig. 4. The agreement of the data with a parabolic form (solid line) means that the wall is steep ($E_P \gg E_S \simeq 0.05$ meV) so that the deviation from a square well is negligible. The inferred well width is $t = 0.3$ μm, in agreement with the lithographic linewidth. The fit also yields a barrier energy $E_b = 13$ meV, which defines the bottom of the potential well relative to $E_F(V_g)$ measured from SdH oscillations.[9,10]

For $B > 0$, the electron is in the electrostatic potential plus a magnetic potential $V_b = m\omega_c^2(x - x_0)^2/2$, where $x_0 = -\hbar k/eB$. For $t = 0$, the new potential is just a shifted parabola, so the solution is a new harmonic oscillator,[21,15] but with a new curvature $\omega = (\omega_c^2+\omega_0^2)^{1/2}$, and an enhanced effective mass $m^* = m\omega^2/\omega_0^2$. The subband bottom rises and eventually approaches the Landau level when $\omega_c \gg \omega_0$. $E(k)$ is still $\propto k^2$ with a mass that increases with B but is independent of n.

For $B > 0$ and $t > 0$,[9] m^* still describes the dispersion curve $E_n(k,B) = E_{noff} + \hbar^2k^2/2m^*$, in the low-$B$ and high-n limit. Since this equation is not necessarily true in the limit $k \to 0$, the significance of E_{noff} (which is the $B = 0$ intercept of the fit) is not clear.[9] One must apply these formulas to the data advisedly since B is not fixed while the dispersion in k is traced, but since the range of B over which each peak is studied is small, we can safely approximate B as a constant in the analysis. The resulting m^* are displayed in Fig. 4. They increase more than 50-fold. For $n = 7$ to $n = 4$, m^* is described quite well by the parabolic field dependence discussed above, but there is significant deviation at higher field where the Landau level is beginning to form. From the fit, we get $m^*(B = 0) = 0.95$ m, in excellent agreement with the ideal value 1; and the electrostatic parameter $\hbar\omega_0 = 0.12$ meV, which is smaller than we had expected given the parabolic dependence of $E_n(0,0)$ on n.

The enhancement of m^* by the magnetic field in 1D subbands has been known theoretically for some time, but, to the best of our knowledge, this is the first experimental measurement for two reasons. First, in the usual ballistic one-dimensional conductance experiments,[15] k and m^* (the density of states) cancel each other and lead to the quantized conductance steps. Second, experiments designed to study the magnetoelectric subbands, usually through the SdH effect, measure the magnetic depopulation of the subbands, and are intrinsically mostly sensitive to the subband bottoms. Except in studies of the sharpening of the depopulation peaks,[9] little attention has been paid to the mass enhancement. In contrast, our sample acts like a small mass spectrometer and provides a direct measurement of the subband dispersion relation and the carrier mass.

Similar measurements were also conducted on a coupled two-ring samples and a single ring with flared ports. The results from these experiments further support our cyclotron trapping mechanism explanation, and these will be discussed in a forthcoming publication.

In conclusion, we remark that we have observed cyclotron trapping effects in a GaAs/Al_xGa_{1-x}As ring. The peaks in $R(B)$, resulting from l_{cn} of *each* subband matching the ring radius, directly yielded $E_n(k_{Fn})$. Calculations for straight channels agreed with the data, if the lateral electric confinement was modeled as a flat bottom plus a parabolic wall. The modeling allowed us to observe

the enhancement of the cyclotron effective mass directly. We also remark that it points the way toward making clean interferometers from these materials, thereby removing the random scattering contributions from the interference patterns.[7]

This work was supported with funding from IBM and the Microelectronics Center of North Carolina. We thank K. Li, V. Long, Y. Wang, and W. Gao for their assistance and M. Büttiker, J. Davies, and H. Baranger for valuable conversations.

[1]J. J. Thompson, Philos. Mag. **44**, 293 (1897).
[2]K. T. Bainbridge, Phys. Rev. **40**, 130 (1932).
[3]Yu. V. Sharvin, Zh. Eksp. Teor. Fiz. **48**, 984 (1965) [Sov. Phys. JETP **21**, 655 (1965)].
[4]V. S. Tsoi, Zh. Eksp. Teor. Fiz. **68**, 1849 (1975) [Sov. Phys. JETP **41**, 927 (1975)].
[5]H. van Houten *et al.*, Phys. Rev. B **39**, 8556 (1989).
[6]D. Weiss *et al.*, Phys. Rev. Lett. **66**, 2790 (1991).
[7]K. Ismail, S. Washburn, and K. Y. Lee, Appl. Phys. Lett. **59**, 1998 (1991); K. Y. Lee *et al.*, J. Vac. Sci. Technol. B **9**, 2834 (1991); S. Washburn, K. Ismail, and K. Y. Lee, in *Quantum Effect Physics, Electronics and Applications*, edited by K. Ismail, T. Ikoma, and H. I. Smith (Hilger, Bristol, 1992).
[8]Since the peak results from guiding of a *single* mode, it is not focusing in the usual sense of optics, where the word refers to the convergence of many such modes. We mention this here to make the connection with magnetic focusing experiments on $GaAs/Al_xGa_{1-x}As$ devices (Ref. 5).
[9]K.-F. Berggren, G. Roos, and H. van Houten, Phys. Rev. B **37**, 10118 (1988); K.-F. Berggren *et al.*, Phys. Rev. Lett. **57**, 1769 (1986); K.-F. Berggren and D. J. Newson, Semicond. Sci. Technol. **1**, 327 (1986).
[10]B. J. van Wees *et al.*, Phys. Rev. B **38**, 3625 (1988); D. A. Wharam *et al.*, *ibid.* **39**, 6283 (1989).
[11]G. Timp *et al.*, Phys. Rev. Lett. **60**, 2081 (1988); C. J. B. Ford *et al.*, *ibid.* **62**, 2724 (1989).
[12]C. W. J. Beenakker and H. van Houten, Phys. Rev. Lett. **63**, 1857 (1989); H. U. Baranger *et al.*, Phys. Rev. B **44**, 10637 (1991).
[13]T. Geisel, R. Ketzmerick, and O. Schedletzky, Phys. Rev. Lett. **69**, 1680 (1992).
[14]B. J. van Wees *et al.*, Phys. Rev. Lett. **60**, 848 (1988); D. A. Wharam *et al.*, J. Phys. C **21**, L209 (1988).
[15]C. W. J. Beenakker and H. van Houten, in *Solid State Physics,* edited by H. Ehrenreich and D. Turnbull (Academic, London, 1991), Vol. 44.
[16]C. J. B. Ford *et al.*, J. Phys. C **21**, L325 (1988); S. Katsumoto, N. Sano, and S. Kobayashi, J. Phys. Soc. Jpn. **61**, 1153 (1992).
[17]The two masses, m_c and m^*, are not the same, but often the two are equal. $m_c(E) = (\hbar^2/2\pi)dA(E)/dE$, where $A(E)$ is the k-space area enclosed by equal-potential E. Invoking a dispersion relation $E_n(k)$ for the tangential wave vector k, and bearing in mind that the equal-potential contour is a circle (because the ring is round), one finds that $m^* = \hbar^2 k/(dE_n/dk)$. See, e.g., J. M. Ziman, *Principles of the Theory of Solids* (Cambridge University, Cambridge, 1986).
[18]P. Exner and P. Seba, J. Math. Phys. **30**, 2574 (1989).
[19]S. E. Laux and F. Stern, Appl. Phys. Lett. **49**, 91 (1986); S. E. Laux, D. J. Frank, and F. Stern, Surf. Sci. **196**, 101 (1988).
[20]D. A. Poole, M. Pepper, K.-F. Berggren, G. Hill, and H. W. Myron, J. Phys. C **15**, L21 (1982).
[21]S. B. Kaplan and A. C. Warren, Phys. Rev. B **34**, 1346 (1986).